A new analytical model for impact and spreading of one drop: application to inkjet printing

FLORENCE GIRARD, PIERRE ATTANÉ AND VÉRONIQUE MORIN

ABSTRACT: The impact of ink drops on glass and three different papers was studied experimentally using a high-speed video camera. An optical arrangement captured top and side views of the impact. Diameter and velocity of the drops were similar to those observed in the inkjet process. In the short term, no penetration into the porous substrate was observed and droplet behavior was qualitatively similar for both plane and porous substrates; however, differences were observed in the maximal wetted area. To help understand these differences, a one-dimensional analytical model was developed to predict the radius of the wetted area shortly after the impact. In our model, kinetic energy and dissipation into the paper mass are estimated in a consistent way. An additional mechanism of dissipation due to the rolling motion near the moving contact line is introduced. The model closely predicts literature data for plane smooth substrates, with an empirical dissipation factor, which is a function of the Ohnesorge number only. Our results show that the dissipation at the moving contact line influences the maximal wetted area and depends upon the nature of the paper.

Application: Drop spreading regimes observed in inkjet printing are analyzed through the extension to porous substrates of a theoretical model for drop impact on impervious substrates.

Modeling of the impact and spreading of one drop on a flat surface has been the subject of continuous effort over the last decade. From the beginning, two approaches have been considered to model the different phenomena involved. The first approach is a numerical simulation of the flow field using a computational fluid dynamics program. Examples are the work by Trapaga and Szekely [1], who studied the impingement of liquid droplets in spraying processes, Fukai et al. [2] and Pasandideh-Fard et al. [3], who studied the influence of wetting and surface tension during the impingement of liquid droplets on flat surfaces, and more recently Toivakka [4], who focused on the spray coating process. The second approach, which we will follow here, is an analytical one. It assumes velocity profiles in a droplet upon impact and applies conservation of mass and energy. Examples are the work of Madjeski [5], Brochard-Wyart and de Gennes [6], Bechtel et al., [7] and Kim and Chun [8].

Recent experimental results can be found in the literature for hydrophilic or hydrophobic non-porous substrates with various degrees of roughness. The first step of our work was to compare those results with the different one-dimensional (1D) analytical models of impact hydrodynamics found in the literature. Finally, the aim of our study is to improve existing models and to propose a new model that can also be used for short-term phenomena occurring in inkjet printing.

MODELING

According to Schiaffino and Sonin [9], the different phenomena that occur during the short time of drop impact can be classified according to two dimensionless numbers, the Weber number (We) and the Ohnesorge number (Oh).

$$We = \frac{\rho d_0 V^2}{\sigma} \tag{1}$$

$$Oh = \frac{\eta}{\sqrt{\rho d_0 \sigma}} \tag{2}$$

where
ρ: density
V: impact speed
d_0: diameter of the drop before impact
η: liquid viscosity
σ: liquid surface tension

These two numbers quantify the relative weight of inertial, viscous, and capillary forces. The Weber number quantifies the forces which drive the spreading, and the Ohnesorge number quantifies the forces which resist the spreading.
All one-dimensional analytical models begin with the same energy balance:

$$\frac{dE_\sigma}{dt} + \frac{dE_c}{dt} + P = 0 \quad \text{or} \quad \frac{dE_\sigma}{dt^*} + \frac{dE_c}{dt^*} + \frac{d_0}{V}P = 0 \tag{3}$$

where
E_σ: surface energy
E_c: kinetic energy
P: rate of dissipation
$t^* = \frac{V}{d_0} t$: reduced time (dimensionless)

Based on this common energy balance, two approaches can be used for analytical modeling. They are distinguished by their assumption regarding the drop shape, which can be considered as either a spherical cap or a cylinder (**Fig. 1**).

Model assuming spherical cap shape

A well-known expression for the variation of surface energy in a spherical cap is:

$$\delta E_\sigma = 2\pi\sigma\left(\cos\theta - \cos\theta_e\right) R\delta R \tag{4}$$

where
θ: contact angle
θ_e: equilibrium contact angle
R: radius of the wetted area

Models found in the literature use many different variables, and direct comparison is therefore difficult. We have therefore transformed the equations to involve the same variables. If the drop shape is considered to be a spherical cap, the dimensionless variable used to characterize the drop evolution is the reduced height of the drop, h*, given by:

$$h^* = \frac{h}{d_0} \tag{5}$$

where
h: height of the drop after impact
d_0: diameter of the drop before impact

All other characteristics of the drop, such as radius and contact angle, are linked to the height by geometrical considerations and volume conservation:

$$R^2 = d_0^{\,2} . \frac{1}{3} . \left(\frac{1}{h^*} - h^{*2}\right) \tag{6}$$

$$\cos\theta = \frac{1 - 4h^{*3}}{1 + 2h^{*3}} \tag{7}$$

If we introduce the reduced height h* (see Equations (6) and (7)) and the initial surface energy $E_{\sigma,0} = \pi\sigma d_0^{\;2}$ into Equation (4), the first term of the energy balance can be expressed as follows:

$$\frac{dE_\sigma}{dt^*} = E_{\sigma,0}\left[\frac{4}{3}h^* - \frac{1}{3}\frac{1}{h^{*2}} + \frac{1}{3}\left(\frac{1}{h^{*2}} + 2h^*\right)\cos\theta_e\right]\frac{dh^*}{dt^*} \tag{8}$$

The common expression of kinetic energy for an axisymmetric flow is:

$$E_c = \frac{1}{2}\rho\int_\Omega \left(U_r^{\;2} + U_z^{\;2}\right) d\Omega \tag{9}$$

where
U_r: radial component of the flow field
U_z: vertical component of the flow field
Ω: drop volume

In order to calculate the kinetic energy, Bechtel et al. [7] considered the flow field to be irrotational. Thus the two components of the flow field are:

$$U_r = -\frac{1}{2}\frac{U_G}{z_G} r \tag{10}$$

$$U_z = \frac{U_G}{z_G} z \tag{11}$$

where
U_G: speed of the mass centre
z_G: height of the mass centre
which can both be expressed in terms of h* by simple geometrical considerations.

If we introduce the initial kinetic energy

$$E_{c,0} = \frac{1}{2}\rho\frac{\pi d_0^{\;3}}{6}V^2$$

, the second term of the energy balance can be expressed as follows:

$$\frac{dE_c}{dt^*} = \frac{d}{dt^*}\left[E_{c,0}\left(\frac{2 + 4h^{*3}}{2h^* + h^{*4}}\right)^2\left(\frac{1}{36}\frac{1}{h^*} + \frac{11}{72}h^{*2} + \frac{13}{90}h^{*5}\right)\left(\frac{dh^*}{dt^*}\right)^2\right] \tag{12}$$

As for the dissipative term of the energy balance, four expressions for this can be found in the literature. For Bechtel et al. [7], dissipation occurs in a shear boundary layer between drop and surface, where the shear stress *f* can be empirically expressed as

$$\tau = \frac{1}{d_0} k\,\eta U_r .$$

The third term of the energy balance can be expressed as follows:

$$P = E_{\sigma,0} Oh\sqrt{We}\,\frac{k}{18}\,\frac{\left(h^{*3}-1\right)^2\left(1+2h^{*3}\right)^2}{h^{*4}\left(2+h^{*3}\right)^2}\left(\frac{dh^*}{dt^*}\right)^2 \tag{13}$$

Another approach is based on the molecular kinetic theory [10] of Eyring as adapted by Blake, which concentrates on the dissipative processes occurring in the vicinity of the advancing contact line, which in turn stem from the attachment of fluid particles to a solid. This theory leads to the following expression of the third term of the energy balance:

$$P = E_{\sigma,0} Oh\sqrt{We}\,\frac{f}{6\sqrt{3}}\,\frac{\left(1+2h^{*3}\right)^2}{h^{*3}\left(h^{*}-h^{*4}\right)^{1/2}}\left(\frac{dh^{*}}{dt^{*}}\right)^2 \quad (14)$$

The hydrodynamic theory developed by Brochard-Wyart and de Gennes [6], among others, is exactly opposite to the molecular kinetic theory: the molecular dissipation at the tip is assumed to be negligible and the dominant losses are considered to be due to hydrodynamic shear flows in the core of the spreading droplet. They assumed that when dissipation occurs, a "lubrication approximation" can be used: the vertical component of the flow field can be neglected and the radial component can be considered as simply parabolic. However, it is well known that lubrication flow, like all flows fulfilling a no-slip condition at the wall, implies a shear-stress singularity at the triple line where solid, liquid, and air meet. To solve this problem, they introduced an adjustable parameter L to obtain the following expression of the third term of the energy balance:

$$P = E_{\sigma,0} Oh\sqrt{We}\,\frac{L}{2\sqrt{3}\arccos\left(\dfrac{1-4h^{*3}}{1+2h^{*3}}\right)}\,\frac{\left(1+2h^{*3}\right)^2}{h^{*3}\left(h^{*}-h^{*4}\right)^{1/2}}\left(\frac{dh^{*}}{dt^{*}}\right)^2 \quad (15)$$

Finally, the McHale and Newton model [11] is similar to the previous one. The only difference lies in that viscous dissipation is modeled here by radial flow within a cone inscribed within the spherical cap, rather than within the whole cap. The expression of the third term of the energy balance can then be simplified to:

$$P = E_{\sigma,0} Oh\sqrt{We}\,\frac{2J_w}{27}\,\frac{\left(1+2h^{*3}\right)^2}{h^{*5}}\left(\frac{dh^{*}}{dt^{*}}\right)^2 \quad (16)$$

with an adjustable parameter J_w.

Model assuming cylindrical shape

If the shape of the drop is considered to be a cylinder, the dimensionless variable used to characterize the drop evolution is the reduced radius of the wetted area, R*:

$$R^{*} = \frac{R}{d_0} \quad (17)$$

where

R: radius of the wetted area

d_0: diameter of the drop before impact.

The expression for the surface energy of a cylinder is:

$$E_\sigma = \sigma\left(\pi R^2 + 2\pi R h_{cyl}\right) - \pi R^2\left(\sigma_S - \sigma_{SL}\right) \quad (18)$$

where

h_{cyl}: cylinder height

σ_S: surface energy of the substrate

σ_{SL}: solid / liquid interfacial tension.

If we introduce

$$\cos\theta_e = \frac{\sigma_S - \sigma_{SL}}{\sigma}$$

, the surface energy can be expressed as follows:

$$E_\sigma = E_{\sigma,0}\left(R^{*2}\left(1-\cos\theta_e\right) + \frac{1}{3R^{*}}\right) \quad (19)$$

The common expression for kinetic energy is given by Equation (9). Depending on the assumption made concerning the flow field, the expressions for the radial and the vertical components will vary. Kim and Chun [8] considered the flow field to be irrotational. Thus the two components of the flow field are:

$$U_r = \frac{1}{R}\frac{dR}{dt}r \quad (20)$$

$$U_z = -2\frac{1}{R}\frac{dR}{dt}z \quad (21)$$

Then the kinetic energy is given by:

$$E_c = E_{c,0}\left(\frac{1}{2} + \frac{1}{27}\frac{1}{R^{*6}}\right)\left(\frac{dR^{*}}{dt^{*}}\right)^2 \quad (22)$$

Madjeski [5] considered the flow field to be a shear flow. Thus the two components of the flow field are:

$$U_r = \frac{2}{Rh_{cyl}}\frac{dR}{dt}r\,z \quad (23)$$

$$U_z = -\frac{2}{Rh_{cyl}}\frac{dR}{dt}z^2 \quad (24)$$

Then the kinetic energy is given by:

$$E_c = E_{c,0}\left(\frac{2}{3} + \frac{1}{45}\frac{1}{R^{*6}}\right)\left(\frac{dR^{*}}{dt^{*}}\right)^2 \quad (25)$$

As for dissipation, Kim and Chun [8] provide an empirical expression based on the existence of a shear boundary layer between drop and surface:

$$P = E_{\sigma,0}\sqrt{Oh}\sqrt{We}\,F_d\left(\frac{dR^{*}}{dt^{*}}\right)^2 R^{*2} \quad (26)$$

with an adjustable parameter F_d.

Taking another approach, Madjeski [5] calculated a rigorous expression of the dissipation without any adjustable parameters:

$$P = 4\,E_{\sigma,0}\,Oh\sqrt{We}\left(\frac{dR^{*}}{dt^{*}}\right)^2\left(3R^{*4} + \frac{2}{3R^{*2}}\right) \quad (27)$$

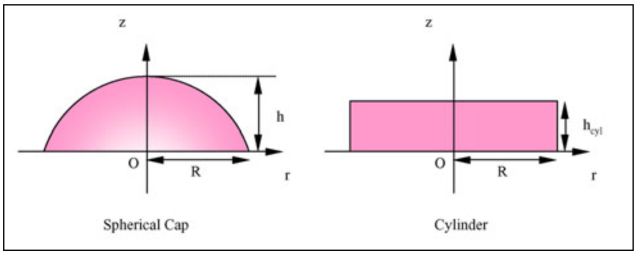

1. Assumption of the drop shape for 1D analytical modeling.

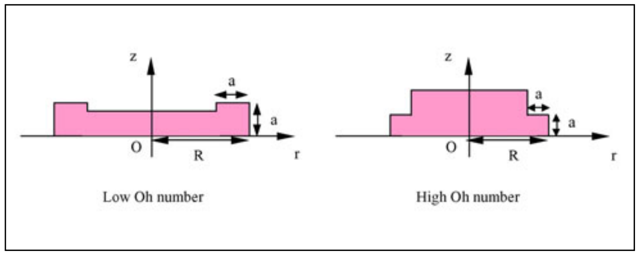

2. Shape of the drop within the proposed model—Cylinder surrounded by a rim.

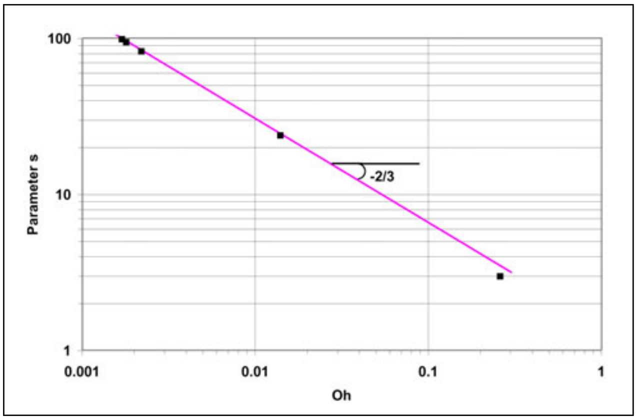

3. Expression of parameter s of the proposed model.

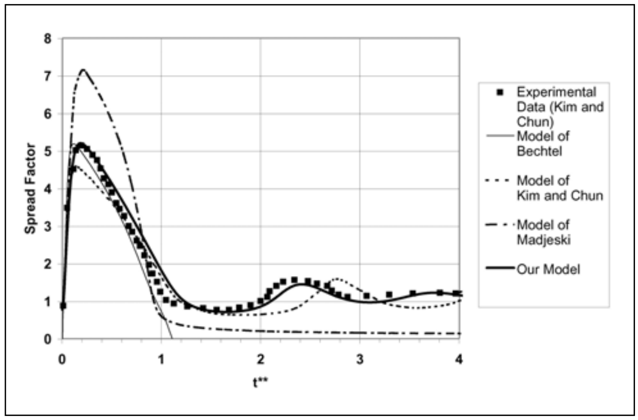

4. Comparison of different 1D analytical models.

Discussion of existing models

The first step in modeling drop impact was the choice of a simple but realistic shape. Examination of numerous experimental results [12][13] shows that the deposition process gives rise to various complicated drop forms. For moderate to high Weber numbers, just after impact the drop looks like a lamella spreading radially on the substrate and topped by a rigid sphere. When the sphere disappears, the lamella then looks like a disc with a more or less pronounced rim. Depending on the values of Weber number (We) and equilibrium contact angle (θ_e), this disc either spreads monotonically or undergoes a succession of spreading and receding events until the final contact line is defined. For low Weber numbers, the initial lamella is thicker, and capillary waves distort the sphere above it [14]. For very low Weber numbers and high Ohnesorge numbers, a spherical cap drop is observed during the entire process [9]. For small drops, the final equilibrium form is a spherical cap. As the drop approaches this final equilibrium form, the spherical cap approximation is increasingly accurate, and authors studying the final wetting phenomena for low values of equilibrium contact angle generally use the spherical cap approximation [6]. From results found in the literature, it can be concluded that the cylindrical form is the most appropriate when dealing with applications linked to the initial stage of drop impact.

The second step is the choice of a flow field assumption. It should be underlined that the choice of an irrotational deformation implies a slip along the wetted area and very low viscous dissipation in the paper mass. Consequently, when the kinetic energy is derived from an irrotational flow field, the dissipation is estimated assuming the existence of a shear boundary layer [7-8]. Madjeski's approach is consistent with this approach, as the same flow field is used to calculate kinetic energy and dissipation. Little is known about the real flow field within the drop. However, it has been established by Dussan V [15] that, near a moving fluid/solid/gas contact line, the fluid undergoes a rolling motion. None of the flow fields proposed thus far takes account of this physical behavior.

Model development

Based on the assumption of a cylindrical drop shape and a flow field with a shear part and an irrotational part, Madjeski's model avoids the main omissions of other models. However, this flow field does not correctly represent the real fluid motion at the triple line. Pictures of water droplet impacts found in the literature show that, for high Weber numbers (We > 100), the edges of the lamella are thicker than at the center. For liquids with higher Ohnesorge numbers, however, the edges of the lamella are thinner than the center. These phenomena were taken into account in our model: the drop shape was assumed to be a cylinder surrounded by a higher or a thinner rim whose dimensions are $a \times a$ (**Fig. 2**).

We assumed that the rolling motion necessary for the triple line to advance is occurring only in the rim. Therefore, our model is based on Madjeski's model for the deformation

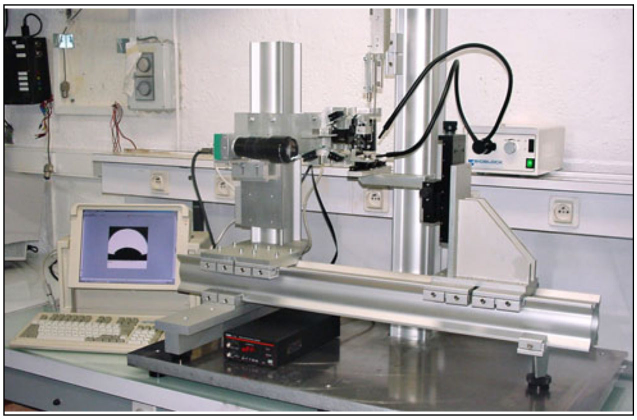

5. ***Drop Measurement Device at CTP.***

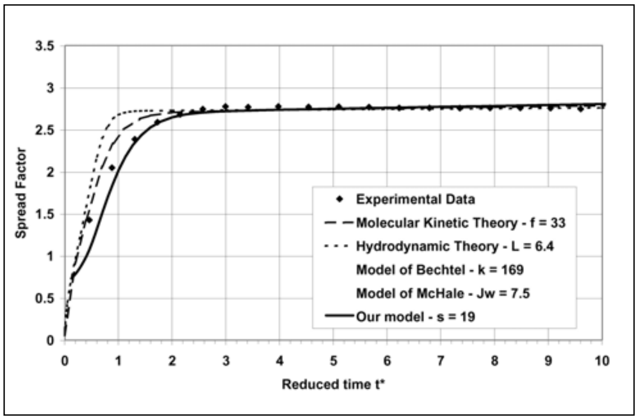

6. ***Comparison of the different models for the experimental data on glass.***

of the bulk of the drop. The first two terms of the energy balance (see Equation (3)) remain the same: surface energy is given by Equation (19) and kinetic energy by Equation (25). The difference lies in the dissipation term. To the dissipation within the cylinder, calculated in Madjeski's model (see Equation (27)), we have added the dissipation within the rim. A dimensional analysis shows that the rim dimension, *a*, does not intervene in the calculation of the power dissipated by the rolling motion:

$$P = \int_{\Omega} \tau \, \gamma \, d\Omega \tag{28}$$

where

$\tau = \eta\gamma$: shear stress

γ: shear velocity.

Assuming that $\frac{a}{2R} << 1$, the volume of the rim is of the order of $2\pi R a^2$. By evaluating the shear velocity in the rim using $\dot{\gamma} = \frac{\sqrt{s}}{a}\frac{dR}{dt}$, the dissipated power in the rim can be expressed as follows:

$$P = 2\, E_{\sigma,0}\, Oh\sqrt{We}\; s\, R^* \left(\frac{dR^*}{dt^*}\right)^2 \tag{29}$$

with an adjustable parameter s.

Thus in our model, the total dissipation within the cylinder surrounded by the rim can be expressed as follows:

$$P = 4\, E_{\sigma,0}\, Oh\sqrt{We} \left(\frac{dR^*}{dt^*}\right)^2 \left(3R^{*4} + \frac{2}{3R^{*2}} + \frac{1}{2} s R^*\right) \tag{30}$$

Our model is based on a dissipation phenomenon in the rim. Since the flow inside this rim is dependent on viscosity, we can assume that the coefficient s depends on the Ohnesorge number. We have therefore applied our model to experimental data in the literature to evaluate the parameter s empirically and express it as a function of the corresponding Ohnesorge numbers.

As shown in **Fig. 3**, we have found a power-law variation of s with Oh. The correlation is perfect, which makes it possible to express the parameter s in the form: $s = 1.41\ Oh^{-2/3}$.

Our model is based on a special drop shape which is only valid for high Weber numbers. In **Fig. 4**, we have reproduced experimental data for the spreading factor $\beta = 2R^*$ according to reduced time $t^{**} = \frac{t^*}{\sqrt{We}}$ from Kim and Chun [8] for We=582, Oh=0.0017 and $\theta_e = 87.4°$. We applied different models to these data: one assuming a spherical cap shape (Bechtel *et al.*), the two models assuming a cylindrical shape (Madjeski, Kim and Chun), and our own model assuming a cylindrical shape surrounded by a rim.

Figure 4 shows that the Bechtel model applied to a spherical cap correctly predicts the decrease of the spreading factor, but then drops to zero, indicating a rebound of the drop, which did not occur. A cylindrical drop shape therefore seems to be a more suitable assumption in this case. Indeed, the correlation of the Kim and Chun model with the experimental data is more satisfactory. However, it is not possible to account for the maximum observed. Moreover, the oscillation frequency of the drop is poorly reproduced. The Madjeski model gives results which are very far from the experimental data. However, it constitutes the basis of the model we have proposed, which gave results very close to the experimental data. Our model, based on assimilating the drop to a cylinder surrounded by a rim, satisfactorily reproduced the two successive maxima and their frequency.

DEVELOPMENT OF A NEW DEVICE

Many devices for studying drop impacts on flat surfaces are described in the literature. Most visualize impact and spreading using one camera angle only. There are three possibilities for viewing, each with its limitations:

- side view: very precise at a short time scale, but provides no information on diffusion within a porous substrate

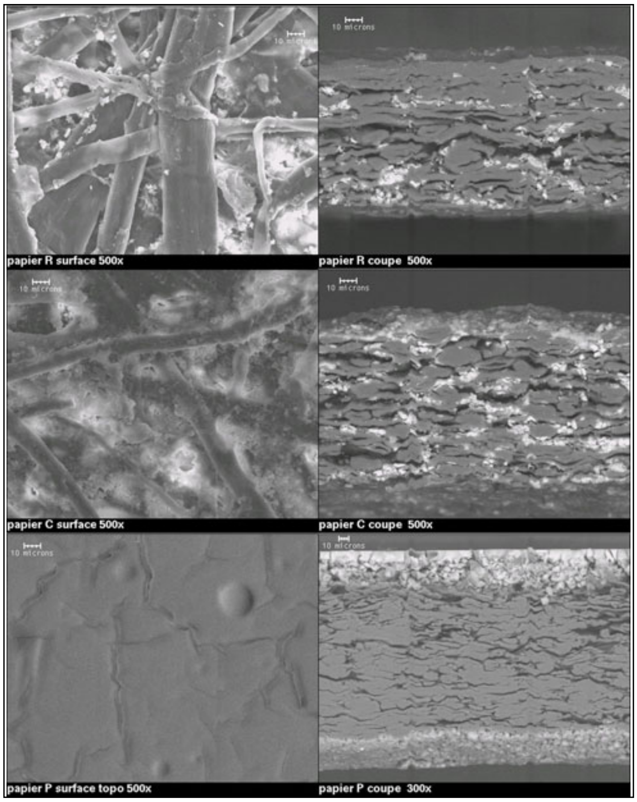

7. SEM photos of selected papers.

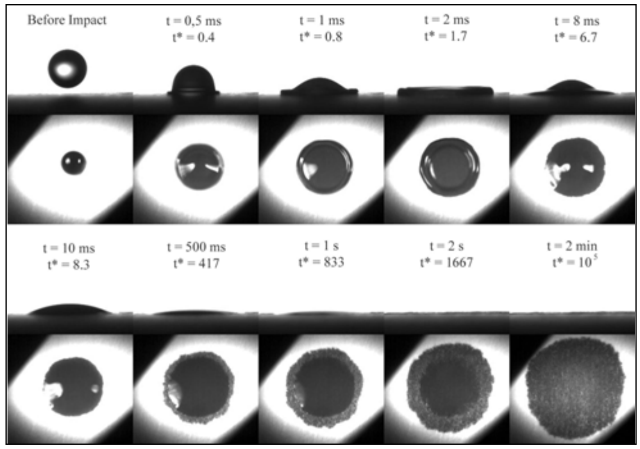

8. Visualization of inkjet ink drop impact on plain paper.

over a longer time scale,

• underside view: useful only for transparent substrates like glass,

• top view: provides a good view of the liquid/substrate contact angle, but correct visualization of spreading at a short time scale is not possible.

Therefore, in order to enable complete study of the impact, penetration, and diffusion of droplets into paper, we developed our own observation device at CTP which combines the advantages of side and top views (**Fig. 5**).

Our device, called the DMD (Drop Measurement Device), is made up of four distinct parts:

• a computer-controlled, motorized syringe,

• a sample plate,

• an optical unit composed of mirrors, lenses, and an optical chopper, which provides two separate optical paths between the drop and the camera. The number of chopper revolutions is synchronized with the camera acquisition speed in order to use the two paths in alternation and thus successively obtain side and top views,

• a high-speed camera with seven-second recording frames at frequencies ranging from 50 frames/s for a resolution of 1280 x 1024 pixels, to 4000 frames/s for a resolution of 120 x 100 pixels.

Image analysis software has been developed to calculate automatically contact angle, diameter, and drop height for side views, spreading and diffusion for top views, and the amount of liquid absorbed, by combining information from the two views. Avi files may be recorded to provide video footage of impacts.

STUDY OF INKJET INK DROP IMPACT

To provide a point of reference, we first studied the impact of several commercial inkjet inks on non-porous substrates such as glass. The observed drops were on a millimeter scale, which is larger than typical inkjet drop sizes. In order to compensate for this size difference, impact speed was reduced to give Weber numbers similar to those encountered in inkjet printing. Rules of similarity produced conclusions which should be applicable to the inkjet process.

Measurements and calculations were carried out with the DMD for the whole process of impact and spreading. However, due to the assumption of a cylindrical drop shape surrounded by a rim, our model applies only to short-term phenomena occurring directly after impact. At longer time scales, the shape of the drop becomes closer to a spherical cap. Therefore, the following results have been limited to one representative, dye-based, magenta ink and a shorter time period of $t^*=10$.

Various properties of the ink, such as surface tension, viscosity, and equilibrium contact angle on glass were measured. The values obtained and used as model parameters were:

Ink density: ρ = 1130 kg/m^3
Ink surface tension: σ = 27.3 mN/m
Ink viscosity: η = 4.2 mPa.s
Equilibrium contact angle: $\theta = 6°$
Diameter of the drop before impact: d_0 = 1.5 mm
Impact speed: V = 1.25 m/s
Weber number: We = 96
Ohnesorge number: Oh = 0.0197.

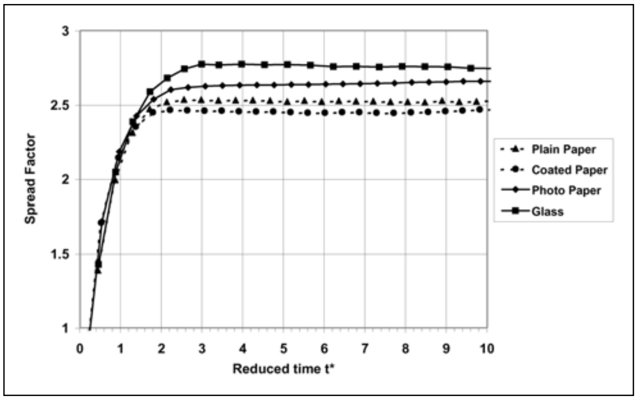

9. Evolution of spreading factor for the experimental data on papers.

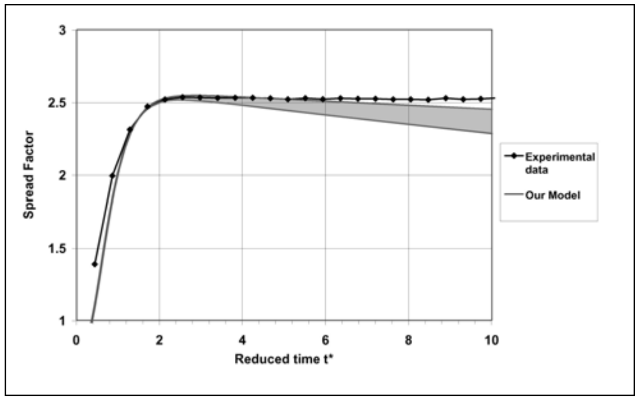

10. Comparison of the proposed model with experimental data — Plain Paper.

Figure 6 shows the evolution of the spreading factor over the shorter time period for our experimental data and that predicted by the different models. For the four models taken from the literature, the corresponding parameters have been adjusted. For impact on glass at short time scales, the Bechtel and McHale models correspond to hydrodynamic theory. Our model reproduces the experimental data at very short time scales in a much more successful manner than the existing models proposed in the literature, without any adjustable parameters (Fig. 6).

In order to test the validity of our model for inkjet printing, three grades of commercial papers were chosen: paper R (a plain paper), paper C (a special inkjet coated paper), and paper P (a high-grade photo paper). SEM micrographs (**Fig. 7**) show the surface (left) and the inner structure (right) of these papers. The coatings were calcium carbonate-based for papers R and C (the second paper having twice as much as the first) and silica-based for the high-grade photo paper.

Figure 8 shows side and top view photos, obtained with the DMD, of the impact of the inkjet ink drop on plain paper. From these photos, one can infer that diffusion within the paper substrate is significant for reduced times t* greater than 10. For further analysis, we chose to use only data collected only during the period of clearly negligible diffusion.

Figure 9 compares the evolution of spreading factors obtained with our DMD for glass and for the three selected papers. This figure shows that the evolution of the spreading factor for reduced time values of 10 and less is qualitatively the same for glass and for papers. This supports the assumption made on the basis of visual inspection of Fig. 8, that diffusion is negligible for the porous substrate up to t*=10.

At this point, the question arose whether the model would be able to reproduce the quantitative differences observed. Since the Ohnesorge number is the same for the four substrates, the model implies that, if the relation $s = 1.41Oh^{-2/3}$ holds, any observed differences would arise from different values of the equilibrium contact angle. This was a serious difficulty, since the equilibrium contact angle is impossible to measure on porous substrates. In the model, we therefore decided to include the advancing contact angle θ_a instead of the equilibrium contact angle θ_e. Indeed, the use of the s value calculated for glass (s = 19, see Fig. 6) and for the three papers gives poor agreement with experimental values. We therefore assumed that the nature of the paper substrate primarily influences the dissipation occurring at the rim, i.e. the parameter s, and sought the s values which would best reproduce the evolution of the spreading factor on the papers.

Values of advancing contact angles and adjusted s parameters are listed in **Table I**.

Paper	θ_a	Adjusted s
Plain Paper	38° ± 5°	22
Special Inkjet Coated Paper	15° ± 3°	26
High-Grade Photo Paper	14° ± 3°	21

I. Values of advancing contact angles and adjusted s parameters.

Figures 10-12 compare our model to experimental data obtained with the DMD on the three grades of paper. The grey areas correspond to the uncertainty resulting from the standard deviation of the advancing contact angle measurements.

When looking at the behavior of the ink on papers where the advancing contact angle is similar to the equilibrium contact angle on glass (i.e. special inkjet coated paper and high-grade photo paper), it can be seen that the model is not very sensitive to the contact angle value. The s values necessary to reproduce correctly the spreading factor values obtained with photo paper were slightly higher (about 10%) than those needed for glass. For the coated paper, a larger increase (about 30%) in the value of s was needed. The model correctly represents the experimental data up to t* values of about 10.

It was concluded that the differences between these

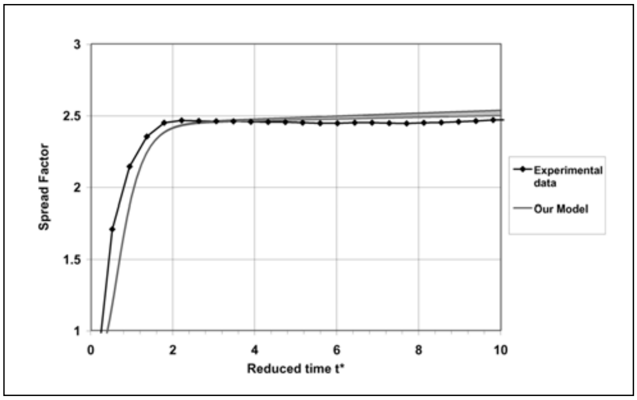

11. Comparison of the proposed model with experimental data—Special Inkjet Coated Paper.

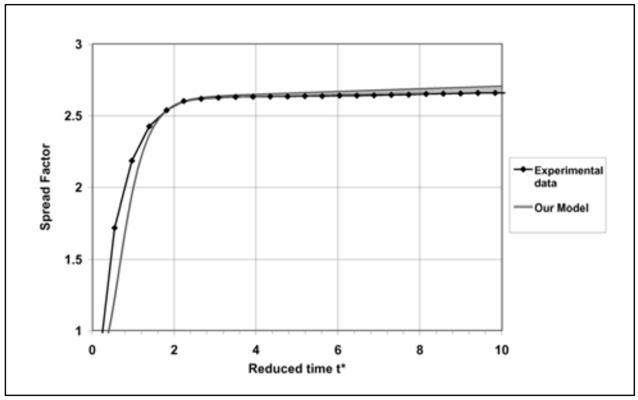

12. Comparison of the proposed model with experimental data—High-Grade Photo Paper.

three surfaces were not limited to the differences in values of the advancing contact angle. Porosity, roughness, or both would therefore be expected to play a specific role, in agreement with the results of Chandra and Avedesian [16].

It is likely that porosity, roughness, or both have an influence on the rolling motion near the triple line. One could expect that dissipation at this triple line would be higher for rough substrates than for smooth; this is precisely in agreement with the results of this research, which generated higher s parameter values for paper than for glass.

CONCLUSIONS

This paper explains the development of a drop impact model based on the variational principle, assuming the droplet form to be a cylinder surrounded by a rim. Influence of the rim on the kinetic energy and surface energy is neglected. Kinetic energy and dissipation in the cylinder are calculated in a consistent way, assuming a flow field fulfilling the no-slip condition on the substrate. The case for the existence of an additional mechanism of dissipation within the rim can be made using the well-known rolling motion observed near the contact line. This additional dissipation is estimated on the basis of dimensional analysis and thus requires the introduction of an empirical parameter. By fitting literature data on the spreading of drops of various viscosities on plane substrates, we found that this parameter could be expressed as a power law function of the Ohnesorge number for smooth substrates.

An experimental device was developed to obtain top and side views of the impact of an ink drop onto glass and papers. Our results show that, directly after impact, the droplet behavior on the four substrates is similar, leading to the conclusion that absorption is not relevant for porous substrates for times up to 10.

One of the major difficulties in applying our model to spreading on paper is the determination of an "equilibrium contact angle." To avoid this problem, we used the advancing contact angle determined at low contact-line velocity. However, to fit the data, it was necessary to increase slightly the value of the rim dissipation parameter s relative to that obtained for the glass substrate. One possible explanation is that porosity, roughness, or both may induce an additional mechanism of dissipation which is absent for smooth non-porous substrates. **TJ**

Submitted: March 1, 2006
Revised: July 18, 2006
Accepted: August 6, 2006

LITERATURE CITED

1. Trapaga, G. and Szekely, J., *Metall. Trans. B*, 22B:901(1991).
2. Fukai, J., Zhao, Z., Poulikakos, D. et al., *Phys. Fluids A*, 5(11):2588(1993).
3. Pasandideh-Fard, M., Qiao, Y.M., Chandra, S. et al., *Phys. Fluids*, 8(6):1344(1996).
4. Toivakka, M., *Proceedings of the 2003 TAPPI 8th Advanced Coating Fundamentals Symposium*, TAPPI PRESS, Atlanta.
5. Madjeski, J., *Int. J. Heat Mass Transfer*, 19:1009(1976).
6. Brochard-Wyart, F. and de Gennes, P.G., *Adv. Colloid Int. Sci.*, 39:1(1992).
7. Bechtel, S.E., Bogy, D.B. and Talke, F.E., *IBM J. Res. Dev.*, 25(6):963(1981).
8. Kim, H.-Y. and Chun, J.-H., *Phys. Fluids*, 13(3):643(2001).
9. Schiaffino, S. and Sonin, A.A., Phys. Fluids, 9(11):3172(1997).
10. de Ruijter, M.J., de Coninck, J. and Oshanin, G., *Langmuir*, 15:2209(1999).
11. McHale, G. and Newton, M.I., *Colloids Surfaces A: physicochemical and engineering aspects*, 206:193(2002).
12. Rioboo, R., Marengo, M. and Tropea, C., *Experiments in Fluids*, 33:112(2002).
13. Sikalo, S., Marengo, M., Tropea, C. et al., *Exp. Therm. Fluid Sci.*, 25:503(2002).
14. Renardy, Y., Popinet, S., Duchemin, L. et al., *J. Fluid Mech.*, 484:69(2003).
15. Dussan V, E.B., *Ann. Rev. Fluid Mech.*, 11:371(1979).
16. Chandra, S. and Avedesian, C.T., *Int. J. Heat Mass Transfer*, 35(10):2377(1992).

INSIGHTS FROM THE AUTHORS

Inkjet technology is a printing process in constant progression. Improvement of printing systems and inks continually challenges the paper industry to develop papers giving better print quality. Many studies on print quality (dot shape, print gloss, bleeding) have shown that it is essential to understand the fundamental phenomena of drop impact and spreading on paper.

The most difficult part of this project was to find a device capable of viewing drop impact and of recording frequencies and duration, especially with the camera angles required for filming the impact. Since nothing suitable was available, we developed our own device, called the Drop Measurement Device (DMD), which records side and top views using only one camera at 4000 ft/s for 7 s.

Of all the findings in this work, the most important is that a simple, one-dimensional, analytical model can predict the radius of the wetted area during the short period after drop impact. The machine and the model, both developed at CTP, should benefit product developers by providing direct information on ink-paper interactions. A possible improvement would be extension of the model to ink-wetted substrate interactions in order to simulate high-frequency inkjet ink droplet ejection.

Girard is a research scientist in the Nanotechnologies and Functional Surfaces Unit at the Centre Technique du Papier (CTP) in Grenoble, France, email Florence.Girard@webctp.com. Attané works as Professor in the Laboratoire de Rhéologie at the Université Joseph Fourier in Grenoble. Morin is the Research and Development Director of the CTP.

Girard

Attané

Morin

AWARD WINNERS ANNOUNCED

The TAPPI 2005 Outstanding Research Paper Award was awarded to Erik Dahlquist, Malardulen University and Andrew Jones, International Paper for their paper "*Presentation of a dry black liquor gasification process with direct causticization*", published in the June 2005 issue of TAPPI JOURNAL Vol. 4, No. 6. The award was presented at the 2006 TAPPI Fall Technical Conference in November 2006. To view the paper visit TAPPI's website at www.tappi.org.

Andy Jones/Erik Dahlquist (L to R).

TAPPI
people resources solutions®
15 Technology Parkway S.,
Norcross, GA, 30092, USA
Address Service Requested